Human Merkel cell polyomavirus small T antigen is an oncoprotein targeting the 4E-BP1 translation regulator

Masahiro Shuda, Hyun Jin Kwun, Huichen Feng, Yuan Chang, and Patrick S. Moore

Cancer Virology Program, University of Pittsburgh, Pittsburgh, Pennsylvania, USA.

Merkel cell polyomavirus (MCV) is the recently discovered cause of most Merkel cell carcinomas (MCCs), an aggressive form of nonmelanoma skin cancer. Although MCV is known to integrate into the tumor cell genome and to undergo mutation, the molecular mechanisms used by this virus to cause cancer are unknown. Here, we show that MCV small T (sT) antigen is expressed in most MCC tumors, where it is required for tumor cell growth. Unlike the closely related SV40 sT, MCV sT transformed rodent fibroblasts to anchorage- and contact-independent growth and promoted serum-free proliferation of human cells. These effects did not involve protein phosphatase 2A (PP2A) inhibition. MCV sT was found to act downstream in the mammalian target of rapamycin (mTOR) signaling pathway to preserve eukaryotic translation initiation factor 4E–binding protein 1 (4E-BP1) hyperphosphorylation, resulting in dysregulated cap-dependent translation. MCV sT–associated 4E-BP1 serine 65 hyperphosphorylation was resistant to mTOR complex (mTORC1) and mTORC2 inhibitors. Steady-state phosphorylation of other downstream Akt-mTOR targets, including S6K and 4E-BP2, was also increased by MCV sT. Expression of a constitutively active 4E-BP1 that could not be phosphorylated antagonized the cell transformation activity of MCV sT. Taken together, these experiments showed that 4E-BP1 inhibition is required for MCV transformation. Thus, MCV sT is an oncoprotein, and its effects on dysregulated cap-dependent translation have clinical implications for the prevention, diagnosis, and treatment of MCV-related cancers.

Introduction

Polyomavirus research has been central to cancer biology (1). Studies on simian vacuolating virus 40 (SV40) T antigen led to the discovery of p53 and uncovered functions for the retinoblastoma tumor suppressor protein (RB1) in cell cycle regulation (2–4). Research on murine polyomavirus led to the discovery of tyrosine phosphorylation (5) and the PI3K signaling pathway (6). More recently, defined elements required for oncogenic transformation of primary human cells has been identified through expression of SV40 T antigens together with h-telomerase reverse transcriptase and activated h-Ras (7, 8).

Merkel cell polyomavirus (MCV) was discovered using digital transcriptome subtraction of Merkel cell carcinoma (MCC) (9). MCC is a clinically aggressive skin cancer that occurs in approximately 1,700 Americans each year, often in individuals with immunosuppression. MCV is clonally integrated into approximately 80% of MCC tumors, but not other common tumors (10–13). MCV is related to the animal tumor virus SV40, and like SV40, MCV T antigens are generated by differential splicing to produce large T (LT), small T (sT), and 57kT antigen proteins (10, 11). sT mRNA shares a common exon 1 with LT, but reads through a splice junction present in LT mRNA to generate a short (18 kDa) alternative reading frame protein possessing unique cellular targeting features.

In tumors, not only is MCV clonally integrated into the tumor cell genome, but it also has various mutations at the 3′ end of the T antigen gene. These mutations eliminate LT viral helicase activity, but are downstream of the sT open reading frame (10, 14). Experimental evidence showing a causal contribution of MCV to MCC tumors comes from knockdown experiments targeting T antigen exon 1, which inhibits expression of all MCV T antigens (15). This knockdown causes cell death and cell cycle arrest only in MCV-positive MCC cell lines, confirming the requirement of MCV T antigens in virus-positive MCC. In MCC tumor biopsies, an MCV LT mAb detects the viral protein in most, but not all, MCV-positive MCC tumors (11). Finally, patient antibodies directed against the common T antigen sequence predict MCC tumor load and recurrence (11, 15, 16).

Although there is little doubt that MCV is a newly described cause of human cancer, nothing is currently known about its mechanisms for cell transformation. Instead, speculation regarding its likely mechanisms must be inferred from related animal polyomaviruses. Polyomavirus T antigens target cell cycle regulatory proteins, and the MCV LT antigen encodes DnaJ and RB1-interacting domains that are unaffected by tumor-specific mutations (10). However, regions of the MCV LT antigen corresponding to those of SV40 LT that bind p53 (2), are frequently lost through tumor-derived mutations.

Polyomavirus targeting of the PI3K-Akt-mTOR signaling pathway (Figure 1) may also contribute to carcinogenesis (8, 17). The MCV sT antigen has a PP2A-interaction domain in its C-terminal region (14) that is similar to those found in other animal polyomaviruses, including the SV40 sT and the murine polyomavirus sT and middle T (MT) (18). Both murine polyomavirus sT/MT and SV40 sT bind the PP2A structural Aα subunit as well as the catalytic C subunit, displacing specific B subunits from the PP2A holoenzyme to inactivate or retarget PP2A enzymatic activity (18–20). SV40 sT activates Akt by preventing its dephosphorylation by PP2A (21, 22). SV40 sT alone is not transforming in rodent cell assays, but it enhances transformation by SV40 LT (23) and contributes to defined oncogene-induced transformation of human cells through PP2A targeting (8).

Conflict of interest: The authors have declared that no conflict of interest exists.

Citation for this article: *J Clin Invest.* 2011;121(9):3623–3634. doi:10.1172/JCI46323.

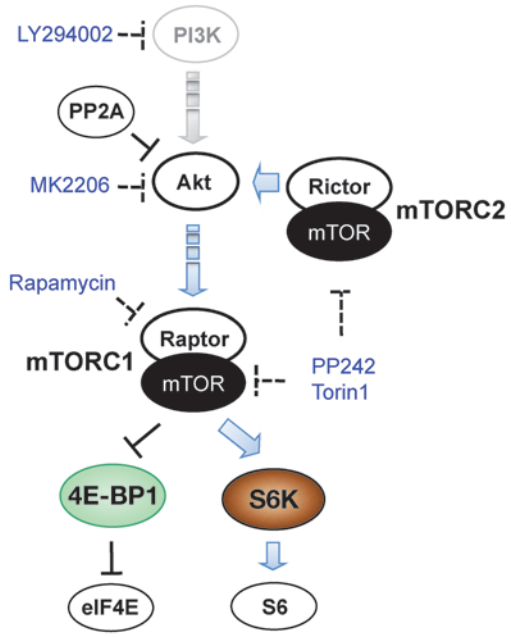

Figure 1
Akt-mTOR pathway. Activities of Akt, mTORC1 (Raptor complex), mTORC2 (Rictor complex), and S6K kinases are shown. mTORC1 phosphorylates and inhibits 4E-BP1, which prevents 4E-BP1 from sequestering the eIF4E cap-dependent translation factor. Kinase inhibitors used in this study are shown in blue, and the respective targets are designated by dotted lines.

Recent studies highlight the importance of cap-dependent translation to tumorigenesis regulated by PI3K-Akt-mTOR signaling (17, 24–26). A key step in cap-dependent translation is the binding of eukaryotic translation initiation factor 4E (eIF4E) to mRNA molecules having a 5′ 7-methylguanosine GTP cap (27). Ribosome recruitment to capped mRNAs is initiated by the assembly of the multisubunit eIF4F, composed of eIF4E, eIF4A, and eIF4G, on the cap. A key regulator of this process is the eukaryotic translation initiation factor 4E-binding protein 1 (4E-BP1), which sequesters eIF4E to prevent eIF4F formation on capped mRNA (28). Induction of cap-dependent translation may play a role in tumor cell growth, since eIF4E overexpression causes rodent cell transformation (29, 30).

4E-BP1 binding to eIF4E is inhibited when 4E-BP1 is phosphorylated by mammalian target of rapamycin (mTOR) kinase. Hyperphosphorylation of 4E-BP1 by mTOR causes 4E-BP1 to release eIF4E, allowing free eIF4E to form the cap assembly and to initiate cap-dependent translation (31). Phosphorylation of 4E-BP1 occurs in a stepwise fashion and involves several sites: first at threonine 37 (T37) and T46 (in humans), priming 4E-BP1 for subsequent hyperphosphorylation at T70, and finally serine 65 (S65) residues by mTOR complex 1 (mTORC1), leading to dissociation of 4E-BP1 from eIF4E (32). Hypophosphorylated 4E-BP1 (α and β forms) migrate faster on polyacrylamide gels than do hyperphosphorylated (γ and δ) forms.

mTORC1-induced 4E-BP1 hyperphosphorylation promotes mitogenesis and cell proliferation, which can be differentiated from other mTORC1 activities (25). For example, phosphorylation of ribosomal protein S6 kinase (S6K), another direct mTOR phosphorylation target, plays a role in cell size and ribosomal biogenesis rather than cell proliferation (25). SV40 sT protein has been reported to dephosphorylate 4E-BP1, possibly by antagonizing mTOR to inhibit cap-dependent translation (33).

In this study, we showed that MCV sT protein was detected in human MCC tumors more commonly than was MCV LT. Knockdown of MCV sT alone retarded MCV-positive cell growth, which indicates that MCV sT expression is required for tumor cell proliferation. We also found that MCV sT behaved very differently from sT proteins reported from other polyomaviruses. MCV sT transformed rodent cells, whereas MCV LT did not. MCV sT–induced transformation was not dependent on MCV sT PP2A or heat shock protein–binding activities. Instead, MCV sT reduced turnover of hyperphosphorylated 4E-BP1, which in turn increased eIF4E activity. Expression of a constitutively active 4E-BP1 that cannot be phosphorylated reversed MCV sT–induced cell transformation, which showed that the proliferative effects of MCV sT are caused by targeting downstream components of the Akt-mTOR pathway. These findings indicate that MCV sT targets cap-dependent translation though a mechanism that contributes to Merkel cell tumorigenesis.

Results

MCV sT protein expression in LT-negative MCC tumors. The CM5E1 mAb, raised against a peptide epitope in sT (Supplemental Figure 1; supplemental material available online with this article; doi:10.1172/JCI46323DS1), distinguished the 18-kDa sT protein from other MCV T antigen isoforms detected by MCV LT–specific (CM2B4; ref. 11) or pan–T antigen–detecting (CM8E6; ref. 14) mAbs (Supplemental Figure 2A). CM5E1 detected endogenous sT protein expression in MCV-infected MCC cell lines (Supplemental Figure 2B), and immunofluorescence showed that it was present in the cytoplasm as well as the nucleus when expressed in 293 cells (Supplemental Figure 2C).

MCV sT antigen was expressed in MCC, and it was more commonly detected than MCV LT antigen in MCV-positive tumors. As shown for case MCCR10-123, sT protein was expressed only in MCC tumor cells and not in adjacent stromal cells (Figure 2A), a staining pattern similar to that of MCV LT (Figure 2B and ref. 11). Of 51 consecutively collected, formalin-fixed and cytokeratin 20–positive (CK20-positive) MCC tumors, 47 (92%) stained positive for MCV sT expression compared with 38 (75%) positive for MCV LT ($P < 0.05$, 1-tailed Fisher exact test; Figure 2G). Only 3 of the 51 MCC tumors (6%) were negative for both MCV LT and sT staining. Among MCCs positive for MCV sT, staining intensities with CM5E1 were reproducible but generally lower than those seen for the 2 tumors in Figure 2. This may reflect low levels of sT expression being typical in MCCs.

Figure 2, D and E, illustrated that some MCC tumors that were positive for MCV DNA were negative for MCV LT protein expression, yet retained expression of the MCV sT. The MCC tumor MCC344 was previously described to be negative for MCV LT antigen expression, although it harbors at least 6 MCV viral genome copies per cell that have been partially sequenced and found to retain the MCV LT mAb epitope sequence (9, 11). This tumor had robust MCV sT antigen staining (Figure 2D), but no staining for MCV LT antigen (Figure 2E). Both cases were negative for SV40 LT expression using the anti–SV40 LT antibody PAb419 as a negative control (Figure 2, C and F). Thus, MCV sT antigen was commonly expressed in MCV-positive tumors, even in a substantial fraction of cases in which MCV LT antigen was not detected.

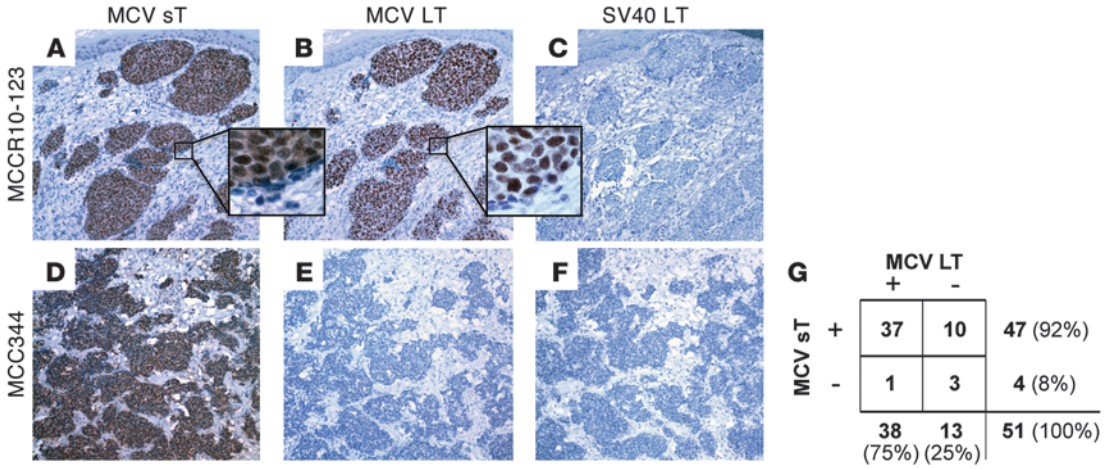

Figure 2

MCV sT antigen protein is commonly expressed in MCC. Immunohistochemical staining of adjacent slides from 2 MCC cases with mouse mAbs to MCV sT (CM5E1 antibody) and MCV LT (CM2B4 antibody) is shown. MCV T antigens were localized only to tumor cells and were not detected in nontumor interstitial tissues. (**A** and **B**) MCC case MCCR10-123, in which both sT and LT were expressed. (**D** and **E**) MCC case MCC344, with abundant sT protein (**D**) but no LT protein (**E**) expression. (**C** and **F**) SV40 LT antigen (PAb419 antibody) was used as a negative control and was not positive for either MCC case. Original magnification, ×100; ×1,000 (insets). (**G**) Blinded analysis of 51 consecutive CK20-positive MCC tumors stained for sT and LT. MCV sT positivity in MCCs, when present, ranged in intensity from slight to robust.

MCV sT is an oncoprotein required for growth of MCV-positive MCC cell lines. We previously showed that shRNA targeting of the common MCV T antigen exon 1 causes pan–T antigen knockdown of both LT and sT and inhibits growth of MCV-infected cell lines (15). As a result of overlapping 3′ coterminal transcripts, LT cannot be readily targeted independent of sT (Supplemental Figure 1). MCV sT mRNA, however, could be knocked down without affecting LT protein expression by targeting the intron 1 sequence (Figure 3A).

A lentiviral shRNA that knocks down only the sT in MCV-positive MKL-1 cells (referred to herein as sT1 shRNA) inhibited MKL-1 cell growth to a similar extent as did shRNA knockdown with an shRNA targeting pan–T antigen exon 1 sequence (referred to herein as pan-T1 shRNA); conversely, control shRNA had no activity (Figure 3B). Proliferation of the virus-negative MCC cell lines UISO and MCC13 was unaffected by either sT or pan–T antigen knockdown (Figure 3B and data not shown), which indicates that this is not due to an off-target effect. Pan–T antigen knockdown was more efficient in inhibiting cell cycle entry, measured by BrdU incorporation, than was sT knockdown alone, but cell cycle progression was also reproducibly diminished by sT targeting in MCV-positive MCC cells (Figure 3C). Knockdown of sT did not cause MCC cell death, as measured by LDH release assays (Figure 3D), in contrast to pan-T knockdown (15). Thus, both MCV LT and MCV sT proteins are likely to separately contribute to MCV-positive MCC tumorigenesis.

Expression of MCV sT, but not MCV LT, results in rodent fibroblast transformation and human fibroblast serum-independent growth. Codon-optimized cDNAs for MCV sT and MCV LT were cloned into lentivirus vectors and expressed in Rat-1 cells. Only sT-expressing cells formed dense foci compared with the empty vector control (32 vs. 0 foci per 60-mm dish; Figure 4, A and B). Truncated, tumor-derived LT cDNAs (LT.339 and LT.350) also did not induce foci formation (Figure 4A). These results were confirmed by an assay for anchorage-independent growth in soft agar (Figure 4C and Supplemental Figure 3A), in which Rat-1 cells were bulk-selected for stable transduction and seeded onto soft agar plates, after which colonies were counted. Rat-1 cells expressing MCV sT readily formed colonies in soft agar, but cells selected for empty vector, full-length LT, or tumor-derived LT remained as nondividing, single cells up to 14 days after plating (Figure 4, C and D, and Supplemental Figure 3, A and B). These results were independently replicated using mouse NIH3T3 cells (Supplemental Figure 3C). Truncated tumor-derived LT proteins induced sparse multicellular aggregates in soft agar, but did not grow into full colonies (Supplemental Figure 3A), which suggests that truncated LT cDNAs have increased cell proliferative capacity compared with the wild-type LT, but, unlike sT, did not fully transform rodent fibroblasts. Dual selection of both sT and tumor-derived LT proteins did not enhance colony formation compared with expression of sT alone (Supplemental Figure 3A). For Rat-1 cells, proliferation was accelerated by expression of MCV sT and, after delay, by LT expression (Supplemental Figure 3D).

MCV sT expression also accelerated human fibroblast proliferation (Figure 5A). BJ fibroblasts immortalized with telomerase reverse transcriptase (BJ-TERT cells) were transduced with MCV sT and grown in 10% or 0% fetal calf serum. In the complete absence of serum, sT expression sustained modest BJ-TERT cell replication, whereas cells infected with empty vector fully arrested and had negligible S-phase entry (Figure 5B). MCV sT expression alone was not able to fully transform human BJ-TERT cells into growth on soft agar (data not shown).

MCV sT-induced cell transformation was independent of PP2A and heat shock protein binding. SV40 sT antigen primarily contributes to cell transformation via targeting of the protein phosphatase PP2A by binding the Aα subunit (20, 34). We found that wild-type MCV sT could also be immunoprecipitated by tagged PP2A Aα (Figure 4E). To examine PP2A's role in MCV sT–induced cell transformation, we generated MCV sT mutants with alanine substitutions at 6 residues that are conserved with known SV40 sT PP2A interaction sites (35). Of the 6 mutations, 4 were unsuitable for additional analysis: alanine substitutions at residue histidine 130 or at a previ-

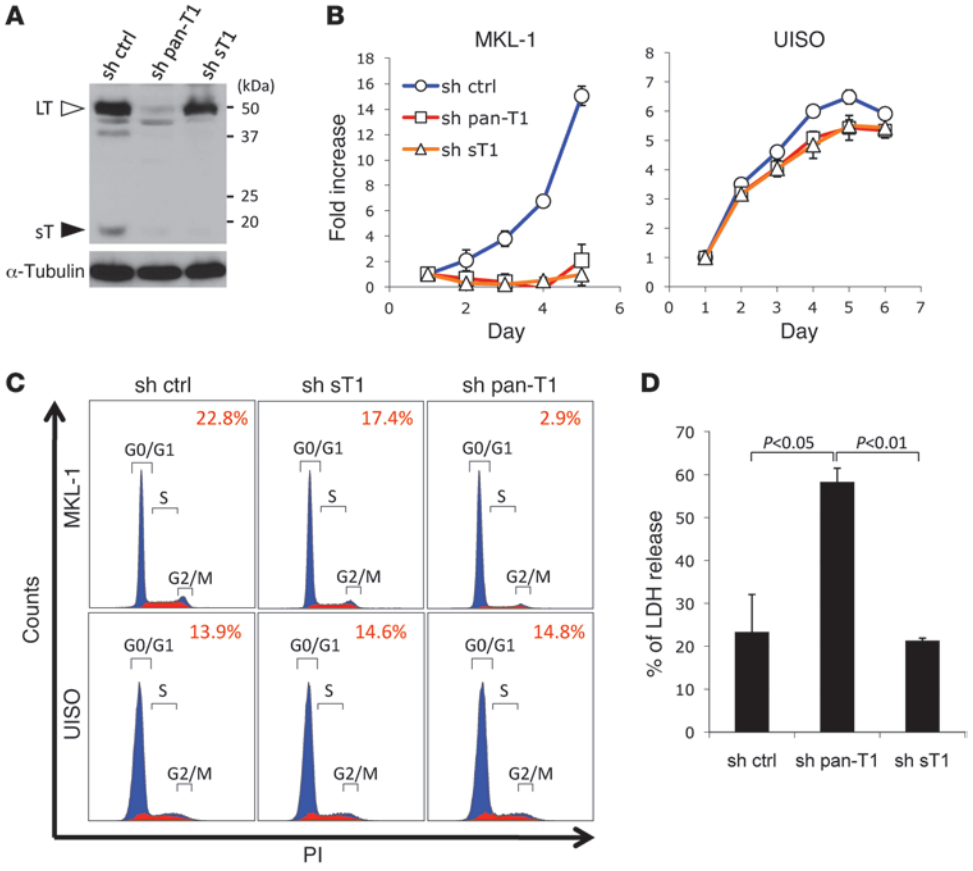

Figure 3

MCV sT expression is required for growth, but not survival, of MCV-positive MCC cells. (**A**) Knockdown with pan-T1 shRNA in MCV-positive MKL-1 cells reduced both LT and sT antigen expression, whereas knockdown targeting with sT1 reduced sT expression alone. sh ctrl, control shRNA. (**B**) Cell proliferation was reduced in MKL-1 cells, but not MCV-negative UISO cells, with both pan-T1 and sT1 shRNA lentivirus transduction (normalized by mean OD values on day 1). (**C**) S and G_2/M phase cell cycle entry, measured by BrdU uptake (red), was markedly reduced by pan-T1 lentiviral knockdown compared with control shRNA for MKL-1 cells, but not UISO cells. Reproducible but modest cell cycle inhibition occurred with sT knockdown in MCV-positive MCC cell lines. Percent cells with BrdU incorporation is indicated within the histograms. PI, propidium iodide. (**D**) sT knockdown did not cause MCC cell death. LDH release was elevated for MKL-1 cells transduced with pan-T1 shRNA lentivirus, indicating increased cell death. No increase in LDH release occurred after sT1 shRNA transduction. Average values for 3 independent experiments are shown.

ously described cysteine 109 residue (14) reduced sT protein stability, whereas substitutions at cysteine 104 and proline 107 did not disrupt PP2A-sT interactions (data not shown). 2 proteins, with alanine substitutions at MCV sT arginine 7 (sT.R7A) or leucine 142 (sT.L142A), were expressed at levels comparable to the wild-type MCV sT protein (Figure 4D), but did not interact with PP2A Aα (Figure 4E). The L142A substitution also prevented MCV sT interaction with PP2A subunit C, whereas R7A did not (data not shown).

Lentiviruses expressing the sT.R7A and sT.L142A proteins had equal or greater efficiency compared with the wild-type sT protein in inducing Rat-1 cell focus formation (46 and 36 foci, respectively, per 60-mm dish; Figure 4A) and anchorage-independent colony formation (Figure 4C). We also examined an sT aspartate-to-asparagine substitution in the exon 1–encoded DnaJ domain, sT.D44N, that eliminates Hsc70 binding to MCV LT (14). The MCV sT protein with this substitution was expressed (Figure 4D) and retained rodent cell transformation efficiency similar to that of the wild-type protein (Figure 4, A and C).

For Rat-1 cells, expression of either sT.R7A or sT.L142A proteins accelerated rodent cell growth similarly to the wild-type sT protein (Supplemental Figure 3D). For human BJ-TERT cells grown in 10% FCS (only sT.L142A was examined), both wild-type and PP2A-binding mutant showed accelerated cell growth compared with cells without sT expression (Figure 5A). BJ-TERT cell mitogenesis with sT.L142A was not significantly reduced compared with wild-type sT for cells grown at 0% FCS. Flow cytometry showed that both sT and sT.L142A initiated increased BJ-TERT cell cycle transit, comparable to the empty vector, under serum-free and serum-complete conditions (Figure 5B). Thus, PP2A interaction is not required for MCV sT to initiate rodent cell transformation or serum-independent human cell proliferation.

MCV sT promotes 4E-BP1 hyperphosphorylation. SV40 sT protein contributes to cell transformation by inhibiting PP2A-dependent Akt dephosphorylation (21, 22). To determine whether MCV sT–induced cell proliferation is also dependent on Akt-mTOR signaling, we examined a downstream target for this pathway, 4E-BP1

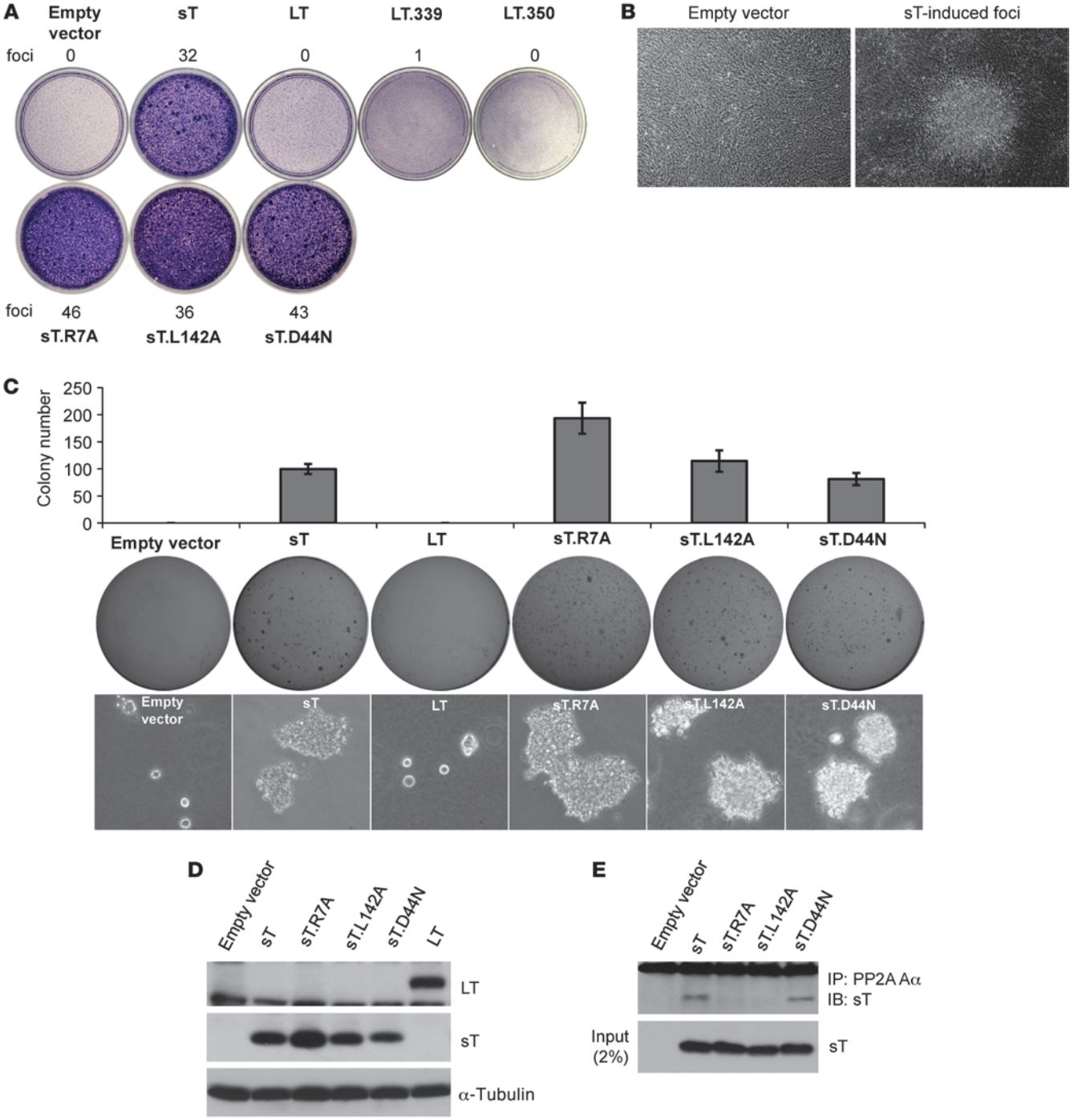

Figure 4

MCV sT induces PP2A-binding and DnaJ domain–independent transformation of Rat-1 cells. (**A**) Lentiviral expression of MCV sT generated dense foci formation in Rat-1 cells compared with empty vector or full-length MCV LT cDNA. Tumor-derived LT antigens (LT.339 and LT.350) also did not increase focus formation. Mutations in the sT PP2A-binding (sT.R7A and sT.L142A) or DnaJ (sT.D44N) domains did not affect focus formation. Number of foci per dish is indicated. (**B**) Phase-contrast images of foci for empty vector– and MCV sT–expressing Rat-1 cells. Original magnification, ×40. (**C**) MCV sT, but not LT, induced anchorage-independent growth of Rat-1 cells in soft agar; this was unaffected by PP2A-binding (sT.R7A and sT.L142A) or DnaJ (sT.D44N) domain mutations. Colonies observed in 6-well triplicates were counted to determine average ± SD colonies per well. Colonies in wells (dark spots) and photomicrographs of typical fields are shown for each condition. Original magnification, ×200. (**D**) LT and sT expression in Rat-1 cells from **C** were detected by immunoblotting with CM2B4 and CM5E1, respectively. (**E**) MCV sT interacted with the Aα subunit of PP2A. HA-tagged PP2A Aα subunit was overexpressed in 293 cells, together with wild-type sT cDNA or with PP2A- or DnaJ-binding mutant cDNAs, and immunoprecipitated with HA antibody. Pulldown of sT protein was detected using anti-sT antibody (CM5E1).

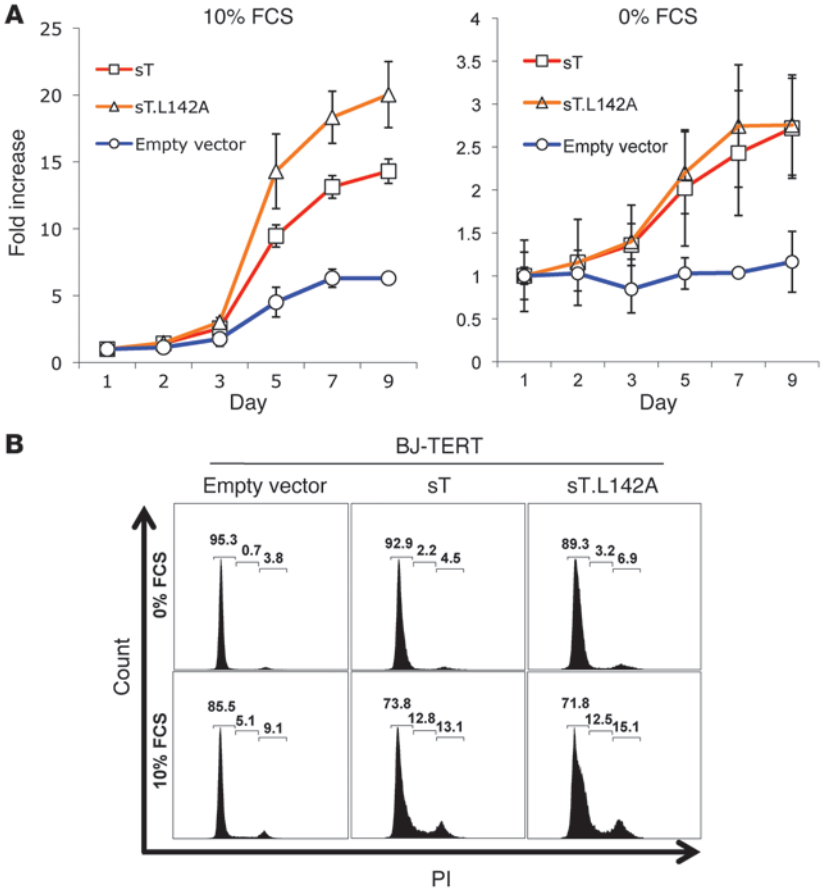

Figure 5
MCV sT promotes serum-independent human BJ-TERT cell proliferation. (**A**) sT protein was transduced by lentiviral vector into immortalized BJ-TERT cells, and cell proliferation was determined in 10% FCS or no serum using a Wst-1 colorimetric cell proliferation assay. sT accelerated BJ-TERT cell growth in the presence of serum and prevented proliferation arrest in the absence of serum (normalized by mean OD values on day 1 for 2 independent experiments performed in triplicate). Mutation of the sT binding site to PP2A (sT.L142A) retained cell proliferation in both the presence and the absence of serum. (**B**) Cell cycle profiles for BJ-TERT cells expressing sT antigens in 0% and 10% FCS. In the absence of serum, greater than 95% of BJ-TERT cells transduced with the empty vector arrested in G_1, whereas substantial fractions of cells expressing wild-type sT (7%) or sT.L142A (11%) continued to transit through the cell cycle.

(Figure 1). As shown in Figure 6A, MCV sT increased 4E-BP1 hyperphosphorylation at S65 (especially for the δ form) in 293 cells but did not markedly change basal phosphorylation (α or β forms, T37/T46). MCV sT expression did not measurably affect raptor expression levels. Long-term raptor (mTORC1) knockdown by selection with a raptor-specific shRNA prevented MCV sT–promoted 4E-BP1 S65 δ phosphorylation (Figure 6A). MCV sT only increased steady-state 4E-BP1 phosphorylation once 4E-BP1 was phosphorylated by mTORC1, which suggests it may prevent turnover of hyperphosphorylated 4E-BP1.

mTOR inhibitor studies provided direct evidence in support of this suggestion. Short-term treatment of 293 cells with the mTORC1-specific inhibitor rapamycin resulted in rapid turnover of the hyperphosphorylated 4E-BP1 phospho-S65 γ form (Figure 6B). Although rapa sortmycin is not a potent inhibitor of 4E-BP1 phosphorylation, the 4E-BP1 phospho-S65 γ form was nearly absent within 15 minutes of the start of rapamycin treatment. MCV sT expression, however, prevented turnover of phospho-S65 for up to 1 hour after treatment (Figure 6B). In contrast to S65 phosphorylation, rapamycin treatment or MCV sT expression did not appreciably alter basal T37/T46 phosphorylation.

Treatment with 2 different active site mTORC1/mTORC2 inhibitors, PP242 (36) or Torin1 (37), for 6 hours also resulted in loss of steady-state S65 hyperphosphorylation (Figure 6C). Unlike rapamycin treatment, basal T37/T46 phosphorylation was nearly abolished after PP242 or Torin1 treatment. When MCV sT was expressed in cells and treated with either PP242 or Torin1, the 4E-BP1 δ form (but not γ form) phospho-S65 (32) was mainly preserved (Figure 6C). Taken together, these data confirmed mTORC1 to be the major kinase hyperphosphorylating 4E-BP1 in the δ form at S65. Phosphorylation was rapidly lost when mTORC1 was inhibited, yet was preserved by expression of MCV sT.

To determine whether MCV sT targeting of the phosphatase PP2A is involved in preserving 4E-BP1 hyperphosphorylation (38), we examined the sT.R7A and sT.L142A proteins in 293 cells in the presence or absence of rapamycin for 1 hour. Both of the PP2A-binding defective sT proteins increased steady-state 4E-BP1 hyperphosphorylation comparable to wild-type MCV sT and were equally resistant to rapamycin (Figure 6D). These data indicate that PP2A targeting is not required for sT-promoted 4E-BP1 hyperphosphorylation.

The effects of MCV sT on 4E-BP1 hyperphosphorylation were confirmed in native MCC cell lines. Both MCV sT and pan-T1 knockdown decreased expression of phosphorylated 4E-BP1, particularly hyperphosphorylated forms, in MKL-1 cells but not in UISO cells (Figure 7A). Similar results were seen for 3 other MCV-positive cell lines (Supplemental Figure 4A). Functional consequences of sT-induced 4E-BP1 hyperphosphorylation were examined using a 7mGTP pulldown assay. Knockdown of either pan-T1 or sT1 in MKL-1 cells decreased eIF4G binding to 7mGTP-resin, comparable to positive control PP242 treatment (Figure 7B). PP242 reduced both eIF4G and eIF4E binding to 7mGTP, and we were unable to determine whether differences between shRNA knockdown and PP242 treatment on eIF4E cap-binding are due to a partial knockdown effect or reflect other biological relevance.

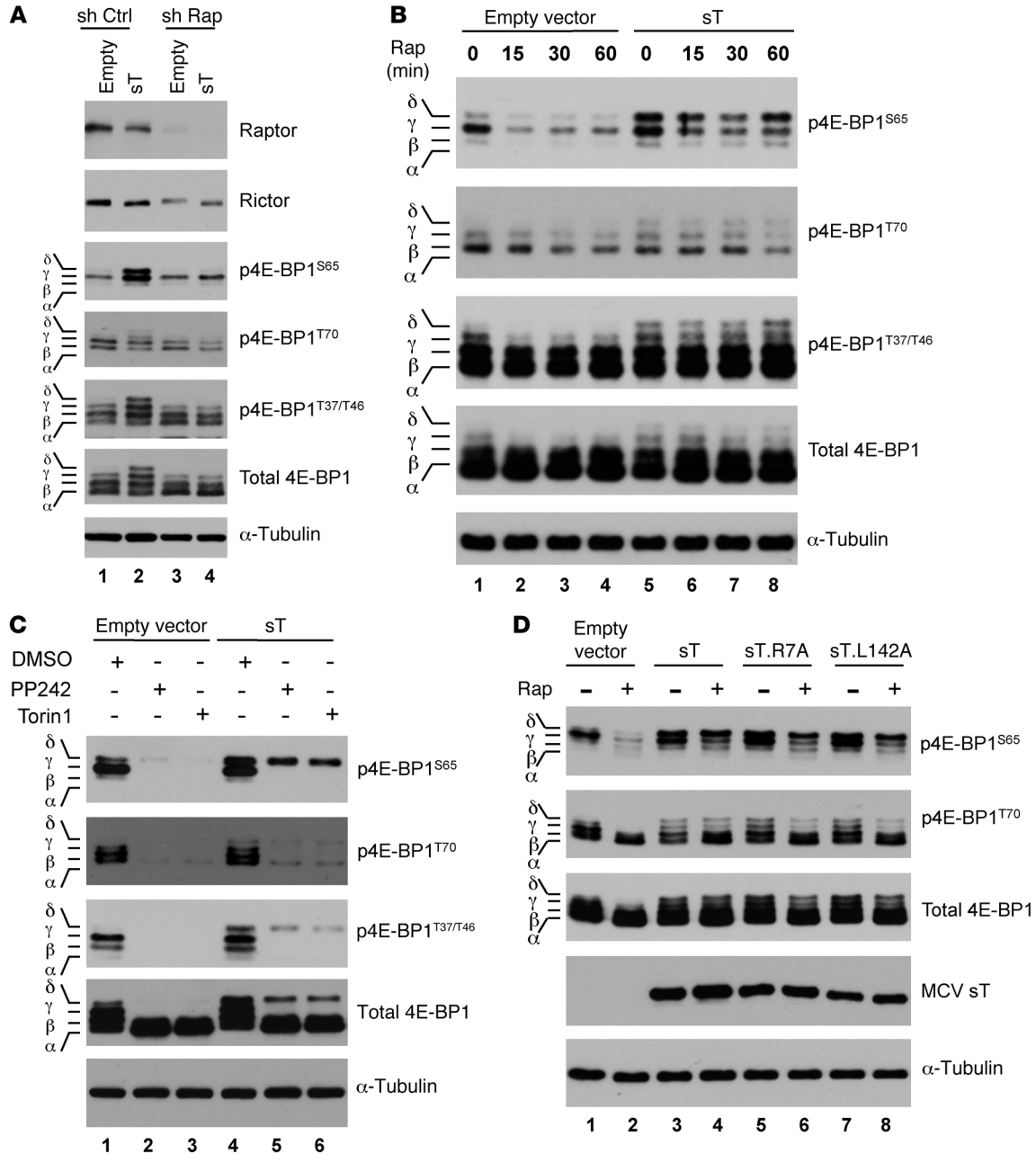

Figure 6

MCV sT promotes 4E-BP1 S65 hyperphosphorylation and cap-dependent translation. (**A**) MCV sT promoted δ 4E-BP1 hyperphosphorylation at S65; this phosphorylation was mediated by mTORC1 and could be inhibited by long-term raptor knockdown. 293 cells were stably transduced with Raptor shRNA lentivirus (shRap) and transfected with sT or empty vector on day 5 after transduction. (**B**) MCV sT prevented loss of hyperphosphorylated 4E-BP1 S65 during short-term mTORC1 inhibition with rapamycin. 293 cells transfected with empty vector or MCV sT were treated with 50 nM rapamycin for up to 1 hour. Basal phosphorylation at T37 and T46 was unaffected by rapamycin treatment or sT expression. (**C**) MCV sT prevented loss of 4E-BP1 during short-term mTORC1 and mTORC2 inhibition with Torin1 and PP242. 293 cells, with or without sT expression, were treated with Torin1 (500 nM) or PP242 (5 μM) for 6 hours. 4E-BP1 was almost completely dephosphorylated after drug treatment in the absence of sT expression. When sT was expressed, the δ S65 form was preserved. (**D**) Both wild-type sT and PP2A-binding sT mutants promoted rapamycin-resistant 4E-BP1 phosphorylation in 293 cells treated with 50 nM rapamycin for 1 hour.

Effect of MCV sT on other Akt-mTOR pathway proteins. In addition to 4E-BP1, S6K is also an mTORC1 kinase target (39). MCV sT markedly increased steady-state T421/S424 phosphorylation of pp70 S6K in 293 cells (Figure 8A). Rapamycin treatment for 1 hour markedly reduced S6K phosphorylation, which was inhibited by sT expression. However, MCV sT preservation of the S6K phospho-T389 form after rapamycin treatment was much reduced compared with phospho-T421/S424. Mutation of PP2A binding

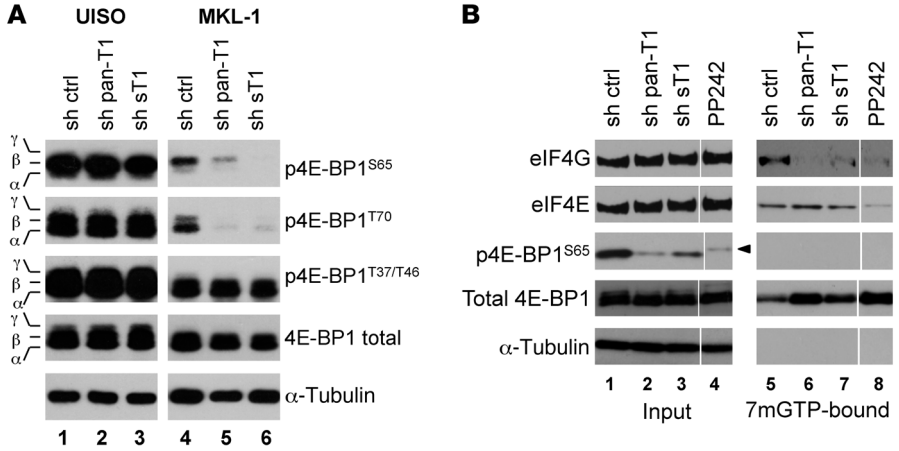

Figure 7

MCV sT knockdown in MCV-infected MCC cells reduces 4E-BP1 hyperphosphorylation and inactivates cap-dependent translation initiation complex formation. (**A**) sT and pan-T antigen knockdown reduced 4E-BP1 γ S65 hyperphosphorylation in MCV-positive MKL-1 cells, but not MCV-negative UISO cells. Priming site T37/T46 phosphorylation was preserved after sT antigen knockdown, whereas secondary sites of phosphorylation (S65 and T70) were markedly reduced. (**B**) Knockdown of either pan-T antigen or sT (by pan-T1 or sT1, respectively) in MKL-1 cells inhibited eIF4G binding to 7mGTP sepharose beads in parallel with loss of 4E-BP1 S65 phosphorylation. Control shRNA–infected MKL-1 cells treated with PP242 are shown as a positive control. Despite partial preservation of 4E-BP1 phospho-S65 (arrowhead) in MKL-1 cells, eIF4E and eIF4G binding was reduced after PP242 treatment. Lanes were run on the same gel but were noncontiguous (white lines).

sites in sT had no effect on its promotion of S6K phosphorylation. S6K's downstream target, S6, showed parallel changes in phosphorylation when MCV sT was expressed (Figure 8A). sT knockdown in native MKL-1 cells confirmed these findings (Supplemental Figure 4B). 4E-BP2, for which phospho-specific antibodies are unavailable, also showed a gel shift in the presence of MCV sT. Like 4E-BP1 hyperphosphorylation and S6K phosphorylation, 4E-BP2 phosphorylation was relatively resistant to rapamycin treatment and was not dependent on sT binding to PP2A (Figure 8A).

To examine the effects of MCV sT on upstream Akt (Figure 1), Akt phospho-S473 was examined in the absence and presence of MCV sT in 293 cells (Figure 8B). No differences in Akt phosphorylation were apparent. PP242 and Torin1 treatment abolished S473 phosphorylation, regardless of MCV sT expression. Furthermore, neither sT.R7A nor sT.L142A PP2A-binding mutants affected Akt S473 phosphorylation (Figure 8C). In MKL-1 cells, Akt was active, as measured by S473 phosphorylation (Figure 8D). Treatment with the PI3K inhibitor LY294002 or the Akt inhibitor MK2206 diminished S473 phosphorylation. T antigen knockdown increased Akt phosphorylation, although this was more pronounced by pan–T antigen knockdown than by knockdown of sT alone. These results indicate that although MCV sT bound some PP2A isoforms (Figure 4E), Akt does not appear to be activated by MCV sT interaction with PP2A, unlike SV40 sT (21, 22).

4E-BP1 hyperphosphorylation is required for MCV sT–induced cell transformation. We expressed sT together with either wild-type 4E-BP1 or 4E-BP1AA (40) in Rat-1 cells and assayed transformation by soft agar assays. 4E-BP1AA is a constitutively active 4E-BP1 with alanine substitutions at the priming T37 and T46 phosphorylation sites. 10 microscopic fields were assessed for each condition by an investigator blinded to the expression conditions.

As was previously found (Figure 4C), Rat-1 cells expressing MCV sT reproducibly formed numerous large, multicellular colonies after 3 weeks of growth in soft agar (Figure 9, A and B). When 4E-BP1 was coexpressed, large colony counts per field were reduced greater than 50%. Large colonies were nearly absent when 4E-BP1AA was expressed together with MCV sT, with most cells remaining as single cells or consisting of clumps of few and scattered cells (Figure 9, A and B). Neither 4E-BP1 nor 4E-BP1AA affected cell viability (data not shown).

Discussion

MCV sT induces loss of contact inhibition, anchorage-independent growth, and serum-independent growth. It is expressed in nearly all MCV-positive MCC tumors and required for the proliferation of MCC tumor cells. MCV sT is an oncoprotein in humans and has potential for use as a diagnostic marker and therapeutic target for MCC.

MCV is related to SV40 and shares similar gene structures, but these 2 viruses differ in their carcinogenic mechanisms. SV40 LT induces cell transformation, whereas MCV LT does not. MCV sT alone is sufficient to cause transformation in rodent cell assays, but this is not the case for SV40. PP2A interaction is critical for SV40 sT and murine polyomavirus sT– and middle T–induced proliferation (8, 18, 19, 41, 42), but PP2A interaction can be abolished in MCV sT without affecting rodent cell transformation, human cell serum–independent growth, or 4E-BP1 phosphorylation.

The mechanism of MCV sT maintenance of 4E-BP1 hyperphosphorylation may provide new insights into Akt-mTOR signaling. Determining how MCV sT does this can only remain speculative until its cellular partners have been more fully described. MCV sT has no recognizable kinase domains and it acts on phosphorylation sites in both 4E-BP1 and S6K, the proximal substrates for mTORC1 kinase. MCV sT preserved 4E-BP1 hyperphosphorylation, particularly of the phospho-S65 δ form; our raptor knockdown revealed that mTORC1 must be active for MCV sT to achieve this effect. It is unlikely, for example, for sT to activate a non-mTORC1 kinase to phosphorylate 4E-BP1.

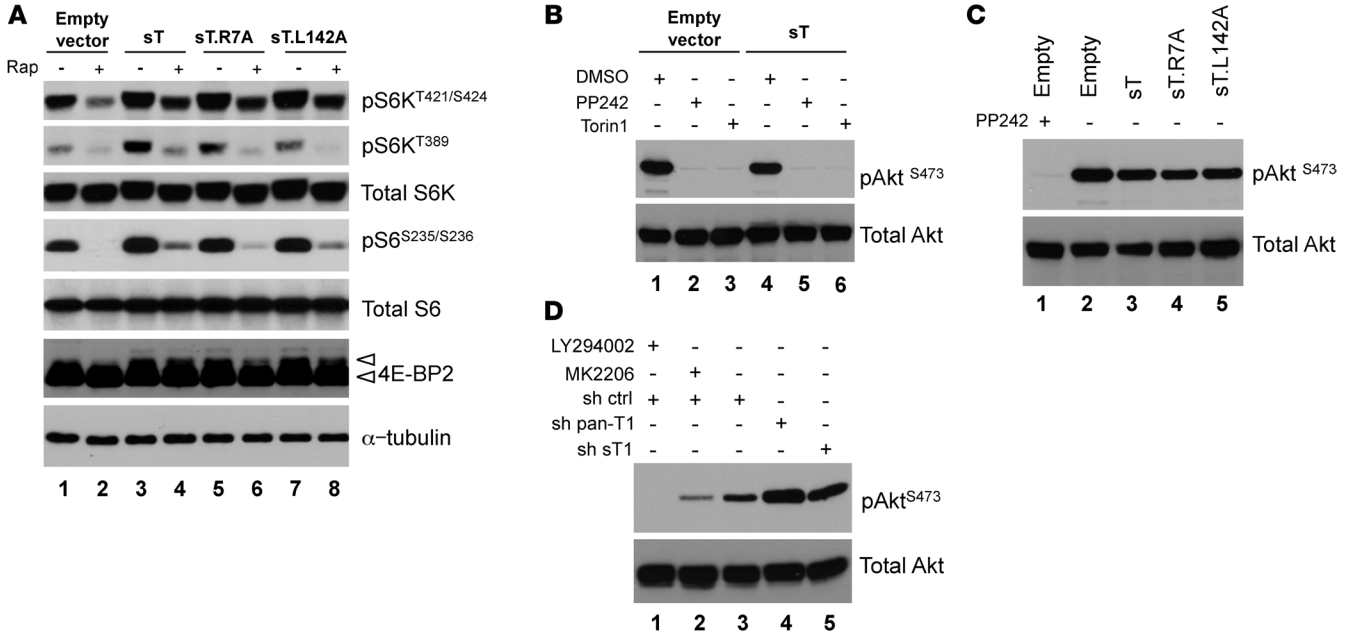

Figure 8

sT promotes steady-state phosphorylation of other mTORC1 downstream molecules. (**A**) sT and PP2A-binding mutants of MCV sT (sT.R7A and sT.L142A) increased steady-state phosphorylation of the S6K kinase at amino acid T389 and T421/S424, its S6 ribosomal protein substrate at S235/S236, and the 4E-BP2 protein (arrowheads). Phosphorylation promoted by sT was relatively resistant to 1 hour rapamycin treatment, except at the S6K T389 site. α-Tubulin was used as a loading control. (**B**) sT, sT.R7A, and sT.L142A did not promote S473 Akt phosphorylation. sT did not prevent PP242 or Torin1 from blocking mTOR-dependent Akt phosphorylation. (**C**) PP2A targeting by MCV sT did not promote Akt phosphorylation. (**D**) MKL-1 cells were transduced with sT1, pan-T, or scrambled shRNA vector lentiviruses for 6 days, and then cell lysates were harvested for immunoblotting. The PI3K inhibitor LY294002 and the Akt inhibitor MK2206 were used as positive controls to show constitutive Akt activity in MKL-1 cells. Akt phosphorylation was increased by both pan-T1 shRNA and sT1 shRNA knockdown.

Hyperphosphorylated forms of 4E-BP1, however, demonstrated quick turnover when cells were treated with mTOR inhibitors, and this turnover was prevented by MCV sT expression (Figure 6C). It is therefore also unlikely that MCV sT activates mTOR complex kinase activity. We do not find a direct interaction between MCV sT and mTOR or 4E-BP1 by coimmunoprecipitation experiments (data not shown).

Our results point toward MCV sT inhibiting 4E-BP1 dephosphorylation or turnover and so elevating steady-state levels of hyperphosphorylated 4E-BP1 (Figure 10). Experiments using Torin1 and PP242 suggested that MCV sT preferentially preserves 4E-BP1 S65 phosphorylation, even when other 4E-BP1 sites are dephosphorylated. We are unaware of a phosphatase or other metabolic protein that regulates both 4E-BP1 and S6K, and so identifying the cellular partner for MCV sT may more generally help to explain how Akt-mTOR signaling is normally turned off. PP2A cannot be responsible for this effect, since PP2A-binding mutations did not affect steady-state 4E-BP1 levels induced by MCV sT.

Our results indicate that deregulated cap-dependent translation through 4E-BP1 hyperphosphorylation may contribute to Merkel cell carcinogenesis. Constitutively active 4E-BP1 that cannot be inactivated by MCV sT prevented sT-induced cell transformation. Whether increased phosphorylation of S6K and other 4E-BP proteins by MCV sT is also required for transformation remains to be examined. These findings have potential therapeutic implications. Akt-mTOR activation is common for other tumor viruses that target upstream components of the Akt-mTOR signaling cascade (43) and are highly sensitive to mTOR inhibitors (44). MCV sT, in contrast, was active downstream of mTOR. Consistent with this, rapamycin had little activity on MCC cell line survival or proliferation at micromolar concentrations (R. Arora, Y. Chang, and P.S. Moore, unpublished observations).

Although MCV sT is necessary for MCC, it is not the only viral factor sufficient to cause the tumor. Loss of sT expression does not fully recapitulate pan–T antigen knockdown (15), and MCV sT did not induce full human BJ cell transformation. We found that LT did promote cell proliferation, and in the setting of human tumors, MCV sT was likely to act in combination with other MCV T antigens, immune suppression, and possibly host cell mutations to promote MCC outgrowth.

Viral tumorigenesis is an uncommon, incidental, and accidental consequence of viral infection, and so sT targeting of 4E-BP1 must promote the replication fitness of nontumorigenic MCV. Viruses commonly induce cap-dependent translation through Akt-mTOR manipulation (17). Adenovirus, for example, activates Akt-mTOR signaling to induce 4E-BP1 phosphorylation early in infection (45), and human herpesviruses, including Kaposi sarcoma–associated herpesvirus (46), herpes simplex 1 (40), and cytomegalovirus (47), induce 4E-BP1 phosphorylation during lytic cycle initiation. MCV sT may similarly target 4E-BP1 to augment viral replication and transmission (48), but in doing so, it places the infected cell at risk for carcinogenic transformation (49).

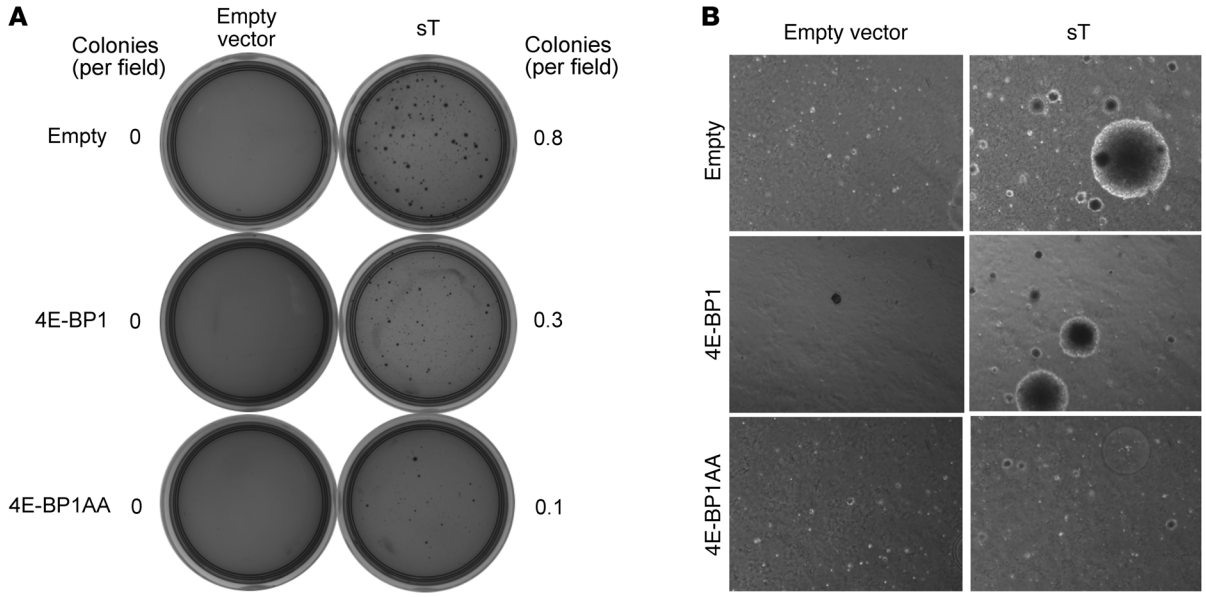

Figure 9
Role of 4E-BP1 phosphorylation in sT-induced transformation. (**A**) Rat-1 cells were stably transduced with empty vector, wild-type 4E-BP1, or constitutively active 4E-BP1AA. Empty vector or MCV sT was then cotransduced into the cells without selection, and they were grown in soft agar for 3 weeks. Colonies were stained with crystal violet, and the colony number per high-power field was determined. (**B**) Phase-contrast images of sT-induced Rat-1 cell colonies in soft agar. Original magnification, ×40.

Methods

Further information can be found in Supplemental Methods.

Clinical samples and immunohistochemistry. Human MCC tissues were obtained through a cohort study at the University of Pittsburgh Medical Center (11). Immunohistochemical staining of paraffin-embedded tissues were performed as previously described with mAbs CM2B4 (1:100) and CM5E1 (1:1,000) (11). SV40 T antigen mAb (PAb419) was used as a control for staining. Staining protocols were as described previously (11). Negative (non-MCC human tumor) and positive (sT- and LT-positive MCC tumor) tissue controls were used. Immunohistochemical results were scored in a blinded fashion by 2 different readers, including an American Association of Pathology board–certified pathologist. sT and LT staining were graded as either negative or positive based on nuclear localization of 3,3-diaminobenzidine colorimetric detection in tumor cells.

Cell lines. 293 (ATCC), 293T (Phoenix-ampho), and 293FT (Invitrogen) cells were maintained in DMEM (Invitrogen) supplemented with 10% FBS. MCC cell lines (MKL-1, MKL-2, MS-1, WaGa, and UISO) were cultured in RPMI supplemented with 10% FBS. WaGa cell lines were obtained from J. Becker (Medical University of Graz, Graz, Austria). Rat-1 cells and NIH3T3 cells were maintained in 5% FBS DMEM and in 10% bovine calf serum DMEM, respectively. BJ-TERT cells were grown in 80% DMEM and 20% Medium 199 (Invitrogen) supplemented with 10% FBS. Rat-1 cells, NIH3T3 cells, and BJ-TERT cells were obtained from O. Gjoerup (University of Pittsburgh, Pittsburgh, Pennsylvania, USA).

Plasmids. Codon-optimized LT and sT antigen sequences were commercially synthesized to avoid potential alternative splicing (DNA 2.0 Inc) and were cloned into pcDNA6 (Invitrogen). sT.R7A, sT.L142A, and sT.D44N were generated by the QuickChange Lightening Site-Directed Mutagenesis kit (Stratagene). See Supplemental Methods for primer sequences and restriction sites for the construction. Retroviral constructs for pBabe.puro, pBabe 4E-BP1.puro, and pBabe 4E-BP1AA.puro, which has alanine substitutions at residue T37/T46 (40), were provided by I. Mohr (New York University, New York, New York, USA).

Lentiviral/retroviral infection. pLVX EF.puro was modified from pLVX-puro vector (Clontech) by replacing CMV promoter with elongation factor-1 (EF) promoter. Codon-optimized MCV LT and sT sequences were then inserted using AfeI and SmaI sites. MCV LT and sT were also cloned into the pSMPUW-hygro vector (Cell Biolabs Inc.) using FseI and PacI restriction sites. Tumor-derived LTs LT.339 and LT.350 were amplified using primers (see Supplemental Methods). For shRNA knockdown, 6 shRNAs targeting sT (intron 1) and 1 shRNA targeting raptor (shRaptor) were designed and cloned into pLKO.1 (Addgene) using AgeI and EcoRI. A control shRNA was obtained from Addgene. Pan-T1, the shT1.puro lentiviral shRNA targeting pan–T antigen exon 1 sequence, was previously described (15). For lentivirus production, 293FT (Invitrogen) cells were used for induction according to the manufacturer's instructions. Lentivirus infection was performed in the presence of 1 μg/ml polybrene. For retrovirus production, 12 μg of retrovirus constructs pBabe empty.puro, pBabe 4E-BP1.wt, or 4E-BP1.AA were transfected to HEK293T phoenix-ampho cells by standard calcium phosphate transfection method. MKL-1 cells infected with control shRNA, pan-T1 shRNA, or sT1 shRNA were selected with puromycin (1 μg/ml) for 4 days after infection. Knockdown was evaluated at day 6 after shRNA transduction. For raptor knockdown experiments, 293 cells transduced with shRaptor were selected with G418 (0.9 mg/ml) for 3 days, seeded in 6-well plates for transfection, and used for DNA transfection experiments. Rat-1 cells infected with Babe retroviral vectors were selected with 2 μg/ml puromycin, followed by LVX lentiviral infection encoding MCV sT for transformation assay.

Immunoblotting, antibodies, and inhibitors. Cells were lysed in buffer (10 mM Tris-HCl, pH 8.0; 0.6% SDS; 2 mM NaF; 2 mM $NaVO_3$) containing protease inhibitors (Roche). The lysate was electrophoresed in SDS-PAGE and transferred to nitrocellulose membrane (Amersham). Primary antibodies were incubated overnight at 4°C, followed by anti-mouse IgG–HRP (Amersham) or anti-rabbit IgG–HRP (Amersham) for 1 hour at room temperature. Signals were detected using Western Lightning plus-ECL reagent (Perkin Elmer). The mouse mAb CM5E1 was generated using standard methods of immunizing mice with the KLH-conjugated peptide (EEYGTLK-DYMQSGYNAR) from intron 1 of MCV T antigen (Epitope Recognition

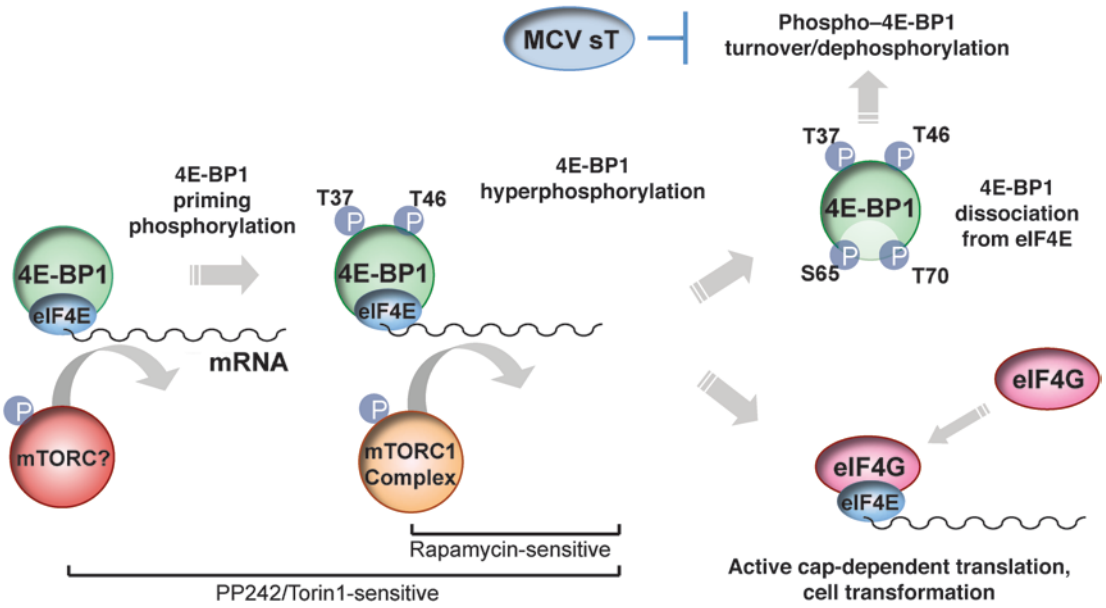

Figure 10
Proposed mechanism of action for MCV sT in cell transformation. MCV sT preserves 4E-BP1 hyperphosphorylation, most likely by preventing hyperphosphorylated 4E-BP1 turnover, which increases cap-dependent protein translation in Merkel cell cancers. The MCV protein does not markedly affect priming 4E-BP1 phosphorylation at residues T37 and T46 and does not directly induce 4E-BP1 phosphorylation.

Immunoreagent Core facility, University of Alabama). The following antibodies were used in this study: CM5E1 (1:1,000), CM2B4 (1:2,500) (11), CM8E6 (1:250) (14), PAb419 (50), 4E-BP1, phospho–4E-BP1$^{T37/T46}$, phospho–4E-BP1^{T70}, phospho–4E-BP1^{S65}, 4E-BP2, pan-Akt, phospho-Akt^{S473}, S6K, phospho-S6K$^{T421/S424}$, phospho-S6K^{T389}, S6, phospho-S6$^{S235/S236}$ (Cell Signaling), and α-tubulin (Sigma-Aldrich). Rapamycin (Sigma-Aldrich), the mTOR active site inhibitor PP242 (Chemdea), Torin1 (provided by D. Sabbatini, Massachusetts Institute of Technology, Cambridge, Massachusetts, USA) and the Akt inhibitor MK2206 (Selleck) were dissolved in DMSO.

Immunoprecipitation. For immunoprecipitation, 293 cells were cotransfected with 5 μg of PP2A Aα subunit (51) and either empty vector or various sT antigen expression vectors (sT, sT.R7A, sT.L142A, and sT.D44N) using Lipofectamine 2000 (Invitrogen). Samples were immunoprecipitated using a previously described protocol (14) with anti-HA mAb (Covance). Immunoblotting was performed using CM5E1 to detect sT.

Cell proliferation assay and cell cycle analysis. Rat-1 (2.0×10^3 cells/well) and BJ-TERT (2.5×10^3 cells/well) cells were seeded in 96-well plates, and Wst-1 cell proliferation assay was performed as described previously (15). OD values were divided by the OD value of day 1 for normalization, and fold increase was used to evaluate cell proliferation. Assays were performed in triplicate. For cell cycle analysis, cells were fixed with 70% ethanol, resuspended in buffer (1% FCS, 0.05 mg/ml propidium iodide, 0.1 mg/ml RNase A in PBS) and incubated for 1 hour at 37°C. For BrdU incorporation studies, MKL-1 cells were labeled with 10 μM BrdU for 3 hours on day 8 after shRNA transduction. BrdU incorporation was detected using Alexa Fluor 488–conjugated mouse anti-BrdU antibody (BD Biosciences — Pharmingen) followed by propidium iodide staining for cell cycle analysis.

Lactate dehydrogenase (LDH) release assay. After lentiviral infection and selection with puromycin, supernatant collected from infected MKL-1 cells with or without addition of Triton X-100 was subjected to LDH release assay (Roche). Percentage of LDH release activity was determined according to the manufacturer's instructions. Results represent the average of 3 independent experiments.

Foci formation assay and soft agar colony formation assay. Rat-1 cells were infected with 100 μl recombinant lentiviruses and grown for 3 weeks for foci formation assay. To determine viral titer and establish stable cell lines, cells were selected with puromycin (2 μg/ml) and hygromycin (300 μg/ml) for pLVX EF and pSMPUW-Hygro lentiviral vectors, respectively. Rat-1 stably expressing MCV T antigens were trypsinized to single cells, counted, suspended in complete medium containing 0.3% agarose (Sigma-Aldrich), and seeded over a 0.6% agar layer in 60-mm dishes (5×10^4 cells/dish). After 3 weeks, colonies were stained with crystal violet (0.025% in PBS), and plates were photographed for soft agar colony formation assay.

Cap-binding assay. MKL-1 cells were lysed in buffer (50 mM Tris-HCl, pH 7.4; 0.15 M NaCl; 1% Triton X-100) supplemented with protease inhibitor (Roche). Lysates (250 μg) were incubated with 50 μl 7-mGTP sepharose 4B (GE Healthcare) for 2 hours at 4°C. Beads were collected, washed, and subjected to immunoblotting. MKL-1 cells treated with PP242 at 5 μM for 6 hours were used as a control.

Statistics. Fisher exact test was performed to determine the significance of differences between sT expression and LT expression in MCC tissues. 2-tailed Student's *t* test was calculated for LDH release assay. *P* values less than 0.05 were considered significant. All data presented in cell proliferation assay and LDH cell death assay are mean ± SD. Representative results of more than 2 independent experiments are shown for cell proliferation assay.

Study approval. All specimens were obtained with patients' informed consent and tested under guidelines approved by the University of Pittsburgh Institutional Review Board (protocol no. 07110141).

Acknowledgments

We thank Ole Gjoerup for providing Rat-1 cells, NIH3T3 cells, and BJ-TERT fibroblasts; Ian Mohr for providing 4E-BP1 and 4E-BP1AA retrovirus constructs; David Sabbatini for providing Torin1; and Jürgen Becker for providing the WaGa cell line. We thank Mary Ann Accaviti for antibody production; Susan

Scudiere for immunostaining; Reety Arora for immunoblotting; Jing Hu for discussions on cap-dependent translation; and Ornette Coleman and Mamie Thant for help with the manuscript. This work was facilitated by UPCI core facilities supported by UPCI Core Facility Cancer Center Support Grant (CCSG) P30 CA047904 and by NIH grants CA136363 and CA120726 to P.S. Moore and Y. Chang, who are also supported as American Cancer Society Research Professors.

Received for publication January 6, 2011, and accepted in revised form June 29, 2011.

Address correspondence to: Patrick S. Moore and Yuan Chang, Cancer Virology Program, University of Pittsburgh Cancer Institute, 5117 Centre Avenue, Pittsburgh, Pennsylvania 15213, USA. Phone: 412.623.7721; Fax: 412.623.7715; E-mail: psm9@pitt.edu (P.S. Moore), yc70@pitt.edu (Y. Chang).

1. Gross L. A filterable agent, recovered from Ak leukemic extracts, causing salivary gland carcinomas in C3H mice. *Proc Soc Exp Biol Med*. 1953;83(2):414–421.
2. Lane DP, Crawford LV. T antigen is bound to a host protein in SV40-transformed cells. *Nature*. 1979;278(5701):261–263.
3. Linzer DI, Levine AJ. Characterization of a 54K dalton cellular SV40 tumor antigen present in SV40-transformed cells and uninfected embryonal carcinoma cells. *Cell*. 1979;17(1):43–52.
4. DeCaprio JA, et al. SV40 large tumor antigen forms a specific complex with the product of the retinoblastoma susceptibility gene. *Cell*. 1988;54(2):275–283.
5. Eckhart W, Hutchinson MA, Hunter T. An activity phosphorylating tyrosine in polyoma T antigen immunoprecipitates. *Cell*. 1979;18(4):925–933.
6. Kaplan DR, et al. Common elements in growth factor stimulation and oncogenic transformation:85 kd phosphoprotein and phosphatidylinositol kinase activity. *Cell*. 1987;50(7):1021–1029.
7. Hahn WC, Counter CM, Lundberg AS, Beijersbergen RL, Brooks MW, Weinberg RA. Creation of human tumour cells with defined genetic elements. *Nature*. 1999;400(6743):464–468.
8. Hahn WC, et al. Enumeration of the simian virus 40 early region elements necessary for human cell transformation. *Mol Cell Biol*. 2002;22(7):2111–2123.
9. Feng H, Shuda M, Chang Y, Moore PS. Clonal integration of a polyomavirus in human Merkel cell carcinoma. *Science*. 2008;319(5866):1096–1100.
10. Shuda M, et al. T antigen mutations are a human tumor-specific signature for Merkel cell polyomavirus. *Proc Natl Acad Sci U S A*. 2008; 105(42):16272–16277.
11. Shuda M, et al. Human Merkel cell polyomavirus infection I. MCV T antigen expression in Merkel cell carcinoma, lymphoid tissues and lymphoid tumors. *Int J Cancer*. 2009;125(6):1243–1249.
12. Kassem A, et al. Frequent detection of Merkel cell polyomavirus in human Merkel cell carcinomas and identification of a unique deletion in the VP1 gene. *Cancer Res*. 2008;68(13):5009–5013.
13. Becker JC, Houben R, Ugurel S, Trefzer U, Pfohler C, Schrama D. MC polyomavirus is frequently present in Merkel cell carcinoma of European patients. *J Invest Dermatol*. 2009;129(1):248–250.
14. Kwun HJ, et al. The minimum replication origin of merkel cell polyomavirus has a unique large T-antigen loading architecture and requires small T-antigen expression for optimal replication. *J Virol*. 2009;83(23):12118–12128.
15. Houben R, et al. Merkel cell polyomavirus-infected Merkel cell carcinoma cells require expression of viral T antigens. *J Virol*. 2010;84(14):7064–7072.
16. Paulson KG, et al. Antibodies to merkel cell polyomavirus T antigen oncoproteins reflect tumor burden in merkel cell carcinoma patients. *Cancer Res*. 2010;70(21):8388–8397.
17. Buchkovich NJ, Yu Y, Zampieri CA, Alwine JC. The TORrid affairs of viruses: effects of mammalian DNA viruses on the PI3K-Akt-mTOR signalling pathway. *Nat Rev Microbiol*. 2008;6(4):266–275.
18. Pallas DC, et al. Polyoma small and middle T antigens and SV40 small t antigen form stable complexes with protein phosphatase 2A. *Cell*. 1990;60(1):167–176.
19. Sontag E, Fedorov S, Kamibayashi C, Robbins D, Cobb M, Mumby M. The interaction of SV40 small tumor antigen with protein phosphatase 2A stimulates the map kinase pathway and induces cell proliferation. *Cell*. 1993;75(5):887–897.
20. Chen W, Possemato R, Campbell KT, Plattner CA, Pallas DC, Hahn WC. Identification of specific PP2A complexes involved in human cell transformation. *Cancer Cell*. 2004;5(2):127–136.
21. Zhao JJ, et al. Human mammary epithelial cell transformation through the activation of phosphatidylinositol 3-kinase. *Cancer Cell*. 2003;3(5):483–495.
22. Rodriguez-Viciana P, Collins C, Fried M. Polyoma and SV40 proteins differentially regulate PP2A to activate distinct cellular signaling pathways involved in growth control. *Proc Natl Acad Sci U S A*. 2006;103(51):19290–19295.
23. Noda T, Satake M, Yamaguchi Y, Ito Y. Cooperation of middle and small T antigens of polyomavirus in transformation of established fibroblast and epithelial-like cell lines. *J Virol*. 1987;61(7):2253–2263.
24. Hsieh AC, et al. Genetic dissection of the oncogenic mTOR pathway reveals druggable addiction to translational control via 4EBP-eIF4E. *Cancer Cell*. 2010;17(3):249–261.
25. Dowling RJ, et al. mTORC1-mediated cell proliferation, but not cell growth, controlled by the 4E-BPs. *Science*. 2010;328(5982):1172–1176.
26. She QB, et al. 4E-BP1 is a key effector of the oncogenic activation of the AKT and ERK signaling pathways that integrates their function in tumors. *Cancer Cell*. 2010;18(1):39–51.
27. Richter JD, Sonenberg N. Regulation of cap-dependent translation by eIF4E inhibitory proteins. *Nature*. 2005;433(7025):477–480.
28. Pause A, et al. Insulin-dependent stimulation of protein synthesis by phosphorylation of a regulator of 5'-cap function. *Nature*. 1994;371(6500):762–767.
29. Lazaris-Karatzas A, Montine KS, Sonenberg N. Malignant transformation by a eukaryotic initiation factor subunit that binds to mRNA 5' cap. *Nature*. 1990;345(6275):544–547.
30. Avdulov S, et al. Activation of translation complex eIF4F is essential for the genesis and maintenance of the malignant phenotype in human mammary epithelial cells. *Cancer Cell*. 2004;5(6):553–563.
31. Beretta L, Gingras AC, Svitkin YV, Hall MN, Sonenberg N. Rapamycin blocks the phosphorylation of 4E-BP1 and inhibits cap-dependent initiation of translation. *EMBO J*. 1996;15(3):658–664.
32. Gingras AC, et al. Hierarchical phosphorylation of the translation inhibitor 4E-BP1. *Genes Dev*. 2001;15(21):2852–2864.
33. Yu Y, Kudchodkar SB, Alwine JC. Effects of simian virus 40 large and small tumor antigens on mammalian target of rapamycin signaling: small tumor antigen mediates hypophosphorylation of eIF4E-binding protein 1 late in infection. *J Virol*. 2005;79(11):6882–6889.
34. Sablina AA, et al. The tumor suppressor PP2A Abeta regulates the RalA GTPase. *Cell*. 2007; 129(5):969–982.
35. Cho US, Morrone S, Sablina AA, Arroyo JD, Hahn WC, Xu W. Structural basis of PP2A inhibition by small t antigen. *PLoS Biol*. 2007;5(8):e202.
36. Feldman ME, et al. Active-site inhibitors of mTOR target rapamycin-resistant outputs of mTORC1 and mTORC2. *PLoS Biol*. 2009;7(2):e38.
37. Thoreen CC, et al. An ATP-competitive mammalian target of rapamycin inhibitor reveals rapamycin-resistant functions of mTORC1. *J Biol Chem*. 2009;284(12):8023–8032.
38. Nanahoshi M, et al. Regulation of protein phosphatase 2A catalytic activity by alpha4 protein and its yeast homolog Tap42. *Biochem Biophys Res Commun*. 1998;251(2):520–526.
39. Jacinto E, et al. Mammalian TOR complex 2 controls the actin cytoskeleton and is rapamycin insensitive. *Nat Cell Biol*. 2004;6(11):1122–1128.
40. Chuluunbaatar U, Roller R, Feldman ME, Brown S, Shokat KM, Mohr I. Constitutive mTORC1 activation by a herpesvirus Akt surrogate stimulates mRNA translation and viral replication. *Genes Dev*. 2010;24(23):2627–2639.
41. Porras A, et al. A novel simian virus 40 early-region domain mediates transactivation of the cyclin A promoter by small-t antigen and is required for transformation in small-t antigen-dependent assays. *J Virol*. 1996;70(10):6902–6908.
42. Sotillo E, Garriga J, Kurimchak A, Grana X. Cyclin E and SV40 small T antigen cooperate to bypass quiescence and contribute to transformation by activating CDK2 in human fibroblasts. *J Biol Chem*. 2008;283(17):11280–11292.
43. Moore PS, Chang Y. Why do viruses cause cancer? Highlights of the first century of human tumour virology. *Nat Rev Cancer*. 2010;10(12):878–889.
44. Stallone G, et al. Sirolimus for Kaposi's sarcoma in renal-transplant recipients. *N Engl J Med*. 2005;352(13):1317–1323.
45. Gingras AC, Sonenberg N. Adenovirus infection inactivates the translational inhibitors 4E-BP1 and 4E-BP2. *Virology*. 1997;237(1):182–186.
46. Arias C, Walsh D, Harbell J, Wilson AC, Mohr I. Activation of host translational control pathways by a viral developmental switch. *PLoS Pathog*. 2009;5(3):e1000334.
47. Kudchodkar SB, Yu Y, Maguire TG, Alwine JC. Human cytomegalovirus infection induces rapamycin-insensitive phosphorylation of downstream effectors of mTOR kinase. *J Virol*. 2004; 78(20):11030–11039.
48. Feng H, et al. Cellular and viral factors regulating merkel cell polyomavirus replication. *PLoS One*. 2011;6(7):e22468.
49. Moore PS, Chang Y. Kaposi's sarcoma-associated herpesvirus immunoevasion and tumorigenesis: two sides of the same coin? *Annu Rev Microbiol*. 2003;57:609–639.
50. Harlow E, Crawford LV, Pim DC, Williamson NM. Monoclonal antibodies specific for simian virus 40 tumor antigens. *J Virol*. 1981;39(3):861–869.
51. Hemmings BA, et al. alpha- and beta-forms of the 65-kDa subunit of protein phosphatase 2A have a similar 39 amino acid repeating structure. *Biochemistry*. 1990;29(13):3166–3173.